

# Finite Element Determination of Thermal Conductivity of SiAlON Ceramics Using Sem Images

İbrahim Uzun, Zühtü Pehlivanlı, Battal Doğan

Department of Mechanical Engineering, Faculty of Engineering, Kırıkkale University, Kırıkkale, 71450 Turkey.  
Phone: +90 (318) 357-4242; Fax: +90 (318) 357-2459, uzun@kku.edu.tr, pehlivanli@kku.edu.tr, dogan@kku.edu.tr

**Abstract** :The thermal conductivity for SiAlON ceramics which are used as a cutting tool material in manufacturing industry has been investigated experimentally, theoretically, and finally numerically. In the experiments, the flash technique was used to determine the thermal conductivity by using the measured thermal diffusion coefficient data in the unsteady regime. Using Maxwell's, serial, and parallel analytical models, the theoretical thermal conductivities have been determined. For the numerical study, the Scanning Electron Microscope (SEM) images of the material were used. From these images, a thermal Ansys® model has been generated through which the effective thermal conductivity was determined. Due to the non-uniformity of the distribution of the boundary phase, different enlargement ratios of the images and as a result finer meshes affect the calculated thermal conductivity values of the ceramics. The experimental and especially the numerical analysis results in this study gave thermal conductivity values which agree quite well with each other.

**Key Words:** Effective thermal conductivity, SiAlON, ceramics, SEM

## I. INTRODUCTION

Thermal conductivities of multi-phase materials has recently emerged as an important subject due to the necessity to produce materials that have better strength and toughness at elevated temperatures. To achieve this, several techniques have been developed recently. The flash technique has been widely used for determining thermal properties over wide ranges of temperatures [1, 2]. In the this technique which is also employed in this study, the front surface of a small sample is subjected to a very short burst of high intensity radiant energy. The resulting temperature rise at the rear surface of the sample is measured and the thermal properties computed from the transient temperature data. There are other approaches such as numerical techniques in literature [3-6] which calculate these properties, but the main change of principle in the numerical analysis carried out in this Kırıkkale University-Faculty of Engineering

study has been the use of real SEM images taken by branding the surface of the material. The microstructure of SiAlON ceramic material is considered as a mixed material. Therefore, changes in the phase structure of a ceramic material affect the average thermal conductivity. The microstructure has also significant importance on thermal conductivity behavior. Although there has been no report on the micro structural effect of  $\alpha$ -SiAlONs, several studies were carried out for Si<sub>3</sub>N<sub>4</sub> materials [7-14]. These studies pointed out that there ia a direct proportion on the grain size and thermal conductivity behavior. Therefore thermal conductivity can be kept under control by means of micro structural modification and the attempt to correlate the microstructures with thermal conductivity behavior play an important role [15, 16]. This can be performed by modeling studies using real microstructure images. However for the application of finite element (FE), the individual intrinsic thermal conductivity values of the consisting phases are required to e calculated.

The thermal conductivity of the particle boundary phase is quite low compared to that of the main phase in the case of SiAlON. Because of this variation, the most important factor affecting the heat conductivity of this material has been found to be the volumetric (or area in our case) ratio of the particle boundary phase which is dispersed in the main phase. The determination of the area ratio from real images is quite hard. But, after transforming the real images to Ansys, these ratios are easily determined. Later the incorporation of the separately available properties of the boundary and the main phases, as well as the boundary conditions of the generated finite element (FE) model, the average thermal conductivity of the SiAlON ceramics is numerically calculated. A rule of mixture type approach can also be used for the theoretical analysis. The superiority of the finite element model over the theoretical model is its ability to take into account the nonuniform boundary phase distribution in the whole area under consideration. Improvement of the mesh size improves the calculated results.

## II. ANALYTICAL SOLUTION

Thermal conductivity of a material varies with respect to temperature, composition, porosity, moisture, and location of the heat source associated with a material. Many theoretical and empirical models have been

reported in literature in order to determine the thermal conductivity of a mixed material, but none of these models is adequate alone. The often used models are known as Series ( $k_s$ ), Parallel ( $k_p$ ), Geometric Mean ( $k_g$ ), and Maxwell and Agari ( $k_x$ ) models. The basic input data in these models are the thermal conductivities and volumetric ratios of the constituent materials. These models are structurally different and depend on the type of material.

The Series and Parallel models provide the lower and upper limits of the thermal conductivity. The Maxwell and Agari model gives good results for low additive ratios. In this study, all the mentioned models have been employed and the results together with the experimentally measured values are presented in Table 1. It can be seen from the Table that the series model has not given good results for SiAlON sample compared to experiment. As the volumetric ratios used in the analytical models are determined from the digital images of the branded surface of the material, variations in the calculated thermal conductivities has been observed depending on the magnification factors employed. The magnification factor has been limited in the interval from 10,000 to 50,000. Better assessment of the effect of this factor has been made through numerical analysis.

TABLE I.  
The thermal conductivity values obtained with different analytical models.

Method	Enlargement ratio $\times 10^{-3}$			
	10	25	30	50
Series ( $k_s$ )	5.78	4.31	4.62	6.25
Parallel ( $k_p$ )	9.29	10.325	10.43	10.86
Maxwell ( $k_x$ )	9.1	9.93	9.96	10.00
Geometric Mean ( $k_g$ )	8.56	9,88	10.00	10.97
Experiment	6.962-8.980			

II. NUMERICAL SOLUTION

The numerical model has been set up by transforming the real SEM image as shown in Figure 1a to the FE model given in Figure 1b. In Figure 1a, the area which is taken as the basis for the FE model is shown as an ellipse. The borders of the main and boundary phases were drawn with absolute lines by conforming to the original as much as possible. In this way, the main and the boundary phase areas which are seen in grey tones in Figure 1a have been clearly formed, and the corresponding area ratios have been determined. These determined areas can be thought of as two different materials having separate physical properties. In this way, the problem has been reduced to a stable regime heat transfer of mixed materials having different properties as well as depending on temperature. The boundary conditions are applied such that there is heat flow only in the horizontal direction and the transverse edges are assumed as adiabatic as shown in

Figure 1a and b. Finally, the FE solution has been obtained using the usual heat transfer procedures.

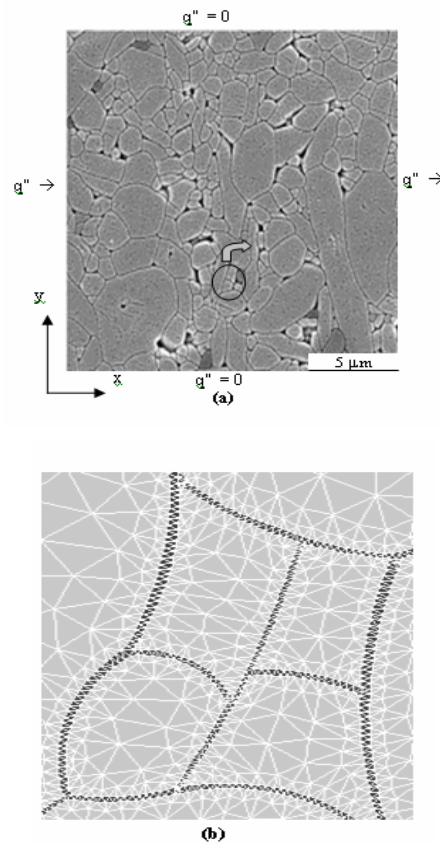


Fig. 1. SEM microstructure photograph (a) and a piece of the transformed numerical model (b).

IV. EXPERIMENTS

Values of thermal conductivity of the SiAlON material have been defined by making use of the thermal diffusivity ( $\alpha$ ) value measured by a Netzsch marked LFA-457 laser flash instrument. Schematic illustration of the experimental setup has been given in Figure 2.

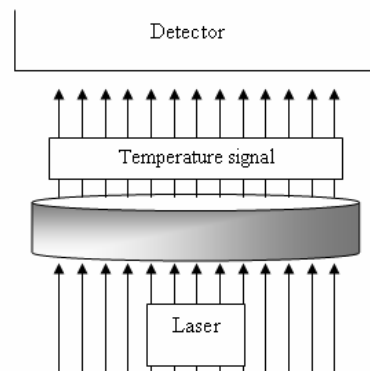


Fig.2. Measurement of thermal diffusivity by laser flash technique.

The thermal conductivity has been determined using the obtained thermal diffusion coefficient, and the density

and the specific heat as  $3.37 \text{ gr/cm}^3$  and  $1 \text{ J/kg.K}$ , respectively. Coefficients of experimental thermal conductivity found at different temperatures together with the numerical and theoretical values have been shown in Table 2. The numerical average values shown in this table are the values obtained from the arithmetic average values of the thermal conductivity obtained at different enlargement ratios. It can be said that the average values conform to the experimental values. It can be seen that the values calculated theoretically at low temperatures show deviations but they approach to the experimental and numerical values obtained at high temperatures. In the numerical calculations, the thermal conductivity of the main phase has firstly been considered as constant and secondly variable with temperature.

TABLE II.  
Experimental, numerical and theoretical thermal conductivity values.

Temperature (K)	Effective Thermal Conductivity ( $k_e$ )		
	Experimental	Numerical	Theoretical
298	8.980	10.332	21.267
373	7.837	8.049	15.489
473	7.376	7.362	13.759
573	7.135	6.868	12.413
673	6.790	6.360	11.160
773	6.611	6.028	10.267
873	6.651	5.869	9.665
973	6.602	5.634	8.959
1073	6.501	5.333	8.148
1173	6.526	5.123	7.481
1273	6.962	5.065	6.872

The effect of different number of nodes in the solution plane on the effective thermal conductivity has been shown in the Figures 3 and 4 depending on the properties being constant and variable, respectively. As the enlargement ratios of SEM images change, the ratios of phase areas also change. It can be said that, it is possible to set a relationship between the area ratios and the effective thermal conductivity, using many images enlarged with different ratios. In this study, effective thermal conductivity has been examined for four different enlargement ratios. It is seen that the effective thermal conductivity of SiAlON increases towards that of the main phase as the enlargement ratio increases. The effective thermal conductivities at different temperature values depending on the enlargement ratios have been shown in Table 3.

Variation of the effective thermal conductivity of the material calculated experimentally, theoretically, and numerically with temperature has been shown in Figure 5.

Although there exists a big difference between the theoretical values and the other, for low temperatures, it is seen that these values approach to each other at high temperatures. In this condition, it can clearly be said that, effective thermal conductivity of the material drops with temperature. Experimental results and numerical results are very close to each other and this result is valid for the whole temperature interval. This situation shows the effectiveness of the numerical study. Figure 6 shows how the effective thermal conductivity ratio (R) is affected by the phase change. As it is expected, increase of the R ratio shows that the effective coefficient approaches to the value of the main phase and the reverse condition shows that it approaches to border phase value. The thermal resistance values at the grain borders are very high due to the value of the thermal conductivity of the particle border phase of the examined material being very low with respect to value of main phase. Depending on this, the magnitude of the thermal flux is greater in the main phase while it is much lower with respect to this value in the border phase. This situation is directly related to the conductivity coefficients. The magnitudes of the thermal flux in an enlarged image examined numerically have been shown in Figure 7.

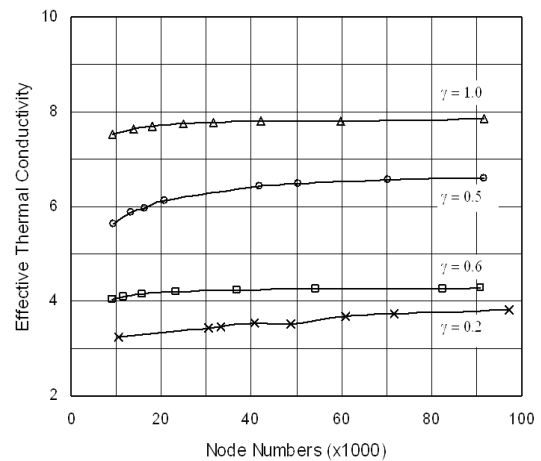


Fig.3. Variability of effective thermal conductivity, for the case where the properties of main phase are constant

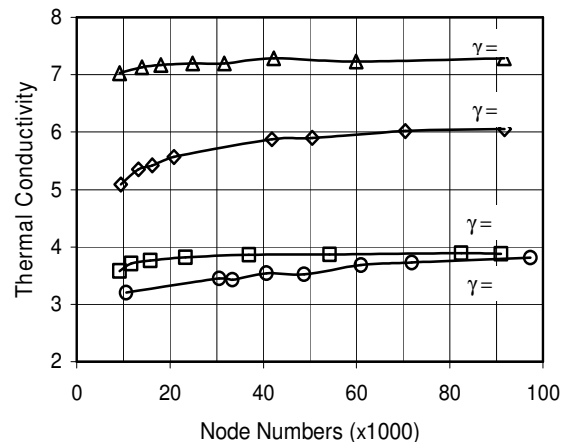


Fig. 4. Variability of effective thermal conductivity coefficient for case where the properties of main phase are variable.

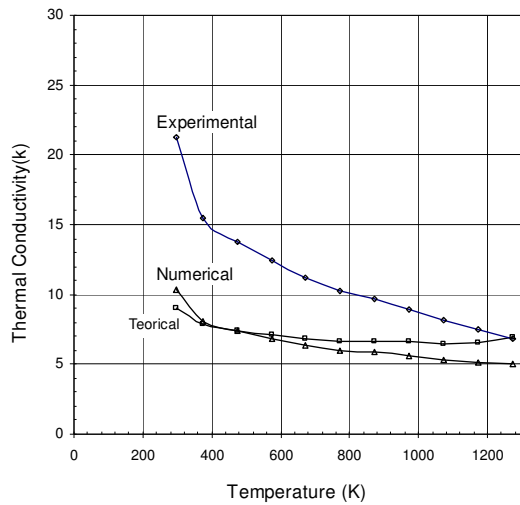


Fig.5. The variability of thermal conductivity coefficient with temperature.

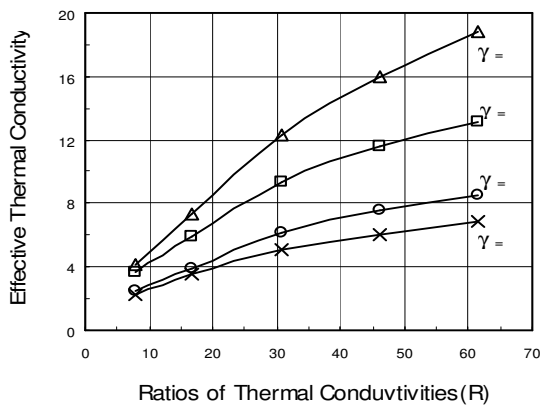


Fig.6. Variability of effective thermal conductivity coefficient depending on the ratios of boundary phase thermal conductivity coefficients

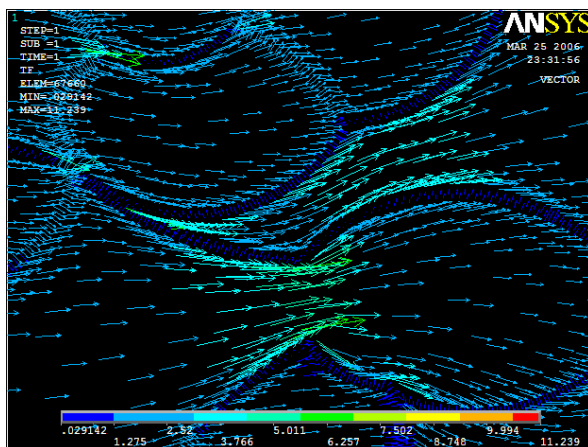


Figure 7. Enlarged vectoral illustration of thermal flux between the phases from any region.

V. DISCUSSIONS AND CONCLUSIONS

Kırıkkale University-Faculty of Engineering

The areas of the main phase and the boundary phases from an image processing at  $2.5 \times 10^4$ ,  $3.0 \times 10^4$ , and  $5.0 \times 10^4$  enlargement ratios of SiAlON have been obtained as 11.31%, 10.27%, and 19.58%, respectively. Depending on these images, triangular shaped finite elements have been used for the formation of the FE model. The reason for this choice is the existence of excessive sharp edges and the thinness of phase lines from place to place. Assuming a constant wall temperature as boundary conditions, the thermal flux and then the thermal conductivity of SiAlON has been determined numerically. The numerical results compare well with the experimental results. Increasing the number of elements in the numerical solution plane does not affect the calculated effective thermal conductivity. The presented study shows the effectiveness of FE modeling in determining accurately the thermal conductivity of multiphase materials.

VI. SYMBOLLS

- $A_m$  Main phase surface area,  $m^2$
- $A_f$  Boundary phase area,  $m^2$
- $c$  Specific heat,  $J/(kg.K)$
- $q''$  Thermal flux,  $W/m^2$
- $k_e$  Effective thermal conductivity,  $W/(m.K)$
- $k_f$  Effective thermal conductivity of boundary phase,  $W/(m.K)$
- $k_s$  Thermal conductivity of series model,  $\left[1/((1-\phi)/k_m + \phi/k_f)\right]$
- $k_g$  Thermal conductivity of geometric model,  $\left[k_m^{(1-\phi)} + k_f^\phi\right]$
- $k_m$  Effective thermal conductivity of main phase,  $W/(m.K)$
- $k_x$  Thermal conductivity of Maxwell and Agari model,  $\left[k_m \cdot \left(\frac{k_f + 2k_m - 2\phi(k_f - k_m)}{k_f + 2k_m - \phi(k_f - k_m)}\right)\right]$
- $k_p$  Thermal conductivity of parallel model,  $\left[(1-\phi)k_m + k_f^\phi\right]$
- $R$  Ratios of main and boundary phase thermal conductivities,  $k_m/k_f$
- $\phi$  Area ratios of main and boundary phase,  $A_m/A_f$
- $\gamma$  Enlargement ratio of microstructure photograph to maximum enlargement
- $\alpha$  Thermal diffusivity,  $m^2/s$

VII. REFERENCES

- [1] S.L. Casto, E.L. Vqalovo, and F. Micari, J. Mech. Working Technology, Vol. 20(1989), 35-46.
- [2] Y. Rong, L. Jia-Jun, L. Bao-Liang, Z. Zhen-Bi, and L. He-Zhuo Miao, Wear, Elsevier, Vol 210(1997), 39-44.
- [3] M.S.S. Baysal, "Effective Thermal Conductivity Coefficient of Mixed Materials Containing Cylindrical Fibers and Particles", Doctorate Thesis, İstanbul Tech. Üniv., (2001)
- [4] I. Tavman, E. Girgin, and R. Klavuz, Proceedings of the 9. Denizli Symposium on Composite Materials, (2002).
- [5] D. Kumlutaş, and I.Tavman, J. Science and Eng., Dokuz Eylül University, Vol. 2(2003), 19-25

- [6] R. Yang, and G. Chen, Physical Review B, Vol 69(2004), 195316/1-10.
- [7] K. Watari, K. Hirao, M. Toriyama and K. Ishizaki, "Effect of Grain Size on the Thermal Conductivity of Si<sub>3</sub>N<sub>4</sub>," J. Am. Ceram. Soc., 82, 777-779 (1999).
- [8] K. Hirao, K. Watari, M. E. Brito, M. Toriyama and S. Kanzaki, "High Thermal Conductivity in Silicon Nitride with Anisotropic Microstructure," J. Am. Ceram. Soc., 79, 2485-2488 (1996).
- [9] N. Hirosaki, Y. Okamoto, F. Munakata and Y. Akimune, "Effect of Seeding on the Thermal Conductivity of Self-reinforced Silicon Nitride," J. Eur. Ceram. Soc., 19, 2183-2187 (1999).
- [10] S. W. Lee, H. B. Chae, D.-S. Park, Y. H. Choa, K. Niihara and B. J. Hockey, "Thermal Conductivity of Unidirectionally Oriented Si<sub>3</sub>N<sub>4</sub>w/Si<sub>3</sub>N<sub>4</sub> Composites," J. Mater. Sci., 35 [18] 4487-4493 (2000).
- [11] N. Hirosaki, Y. Okamoto, M. Ando, F. Munakata and Y. Akimune, "Thermal Conductivity of Gas-pressure Sintered Silicon Nitride," J. Am. Ceram. Soc., 79, 2978-2982 (1996).
- [12] H. Yokota and M. Ibukiyama, "Microstructure Tailoring for High Thermal Conductivity of C-Si<sub>3</sub>N<sub>4</sub> Ceramics," J. Am. Ceram. Soc., 86, 197-199 (2003).
- [13] N. Hirosaki, Y. Okamoto, M. Ando, F. Munakata and Y. Akimune, "Thermal Conductivity of Gas-Pressure Sintered Silicon Nitride," J. Am. Ceram. Soc., 79, 2978-2982(1996).
- [14] K. Watari, K. Hirao, M. E. Brito, M. Toriyama and K. Ishizaki, "Factors to Enhance Thermal Conductivity of C-Si<sub>3</sub>N<sub>4</sub> Ceramics," Advances in Technology of Materials and Materials Processing, 7, 191-202 (2005).
- [15] J. S. Haggerty and A. Lightfoot, "Opportunities for Enhancing the Thermal Conductivities of SiC and Si<sub>3</sub>N<sub>4</sub> Ceramics through Improved Processing," Ceram. Eng. Sci. Proc., 475-487 (1995).
- [16] K. Watari, "High Thermal Conductivity Non-Oxide Ceramics," J. Ceram. Soc. Jpn, 109,7-16 (2001).